Atmospheric
Chemistry
and Physics

Impact of isoprene and HONO chemistry on ozone and OVOC formation in a semirural South Korean forest

S. Kim[1], **S.-Y. Kim**[2], **M. Lee**[3], **H. Shim**[3], **G. M. Wolfe**[4,5], **A. B. Guenther**[6], **A. He**[1], **Y. Hong**[2], **and J. Han**[2,*]

[1]Department of Earth System Science, School of Physical Sciences, University of California, Irvine, CA, USA
[2]National Institute Environmental Research, Incheon, South Korea
[3]Department of Earth and Environmental Sciences, Korean University, Seoul, South Korea
[4]Joint Center for Earth Systems Technology, University of Maryland, Baltimore, MD, USA
[5]Atmospheric Chemistry and Dynamics Laboratory, NASA Goddard Space Flight Center, Greenbelt, MD, USA
[6]Atmospheric Sciences and Global Change Division, Pacific Northwest National Laboratory, Richland WA, USA
[*]now at: Department of Environmental & Energy Engineering, Anyang University, Anyang, South Korea

Correspondence to: S. Kim (saewungk@uci.edu)

Abstract. Rapid urbanization and economic development in East Asia in past decades has led to photochemical air pollution problems such as excess photochemical ozone and aerosol formation. Asian megacities such as Seoul, Tokyo, Shanghai, Guangzhou, and Beijing are surrounded by densely forested areas, and recent research has consistently demonstrated the importance of biogenic volatile organic compounds (VOCs) from vegetation in determining oxidation capacity in the suburban Asian megacity regions. Uncertainties in constraining tropospheric oxidation capacity, dominated by hydroxyl radical, undermine our ability to assess regional photochemical air pollution problems. We present an observational data set of CO, NO_x, SO_2, ozone, HONO, and VOCs (anthropogenic and biogenic) from Taehwa research forest (TRF) near the Seoul metropolitan area in early June 2012. The data show that TRF is influenced both by aged pollution and fresh biogenic volatile organic compound emissions. With the data set, we diagnose HO_x (OH, HO_2, and RO_2) distributions calculated using the University of Washington chemical box model (UWCM v2.1) with near-explicit VOC oxidation mechanisms from MCM v3.2 (Master Chemical Mechanism). Uncertainty from unconstrained HONO sources and radical recycling processes highlighted in recent studies is examined using multiple model simulations with different model constraints. The results suggest that (1) different model simulation scenarios cause systematic differences in HO_x distributions, especially OH levels (up to 2.5 times), and (2) radical destruction ($HO_2 + HO_2$ or $HO_2 + RO_2$) could be more efficient than radical recycling ($RO_2 + NO$), especially in the afternoon. Implications of the uncertainties in radical chemistry are discussed with respect to ozone–VOC–NO_x sensitivity and VOC oxidation product formation rates. Overall, the NO_x limited regime is assessed except for the morning hours (8 a.m. to 12 p.m. local standard time), but the degree of sensitivity can significantly vary depending on the model scenarios. The model results also suggest that RO_2 levels are positively correlated with oxygenated VOCs (OVOCs) production that is not routinely constrained by observations. These unconstrained OVOCs can cause higher-than-expected OH loss rates (missing OH reactivity) and secondary organic aerosol formation. The series of modeling experiments constrained by observations strongly urge observational constraint of the radical pool to enable precise understanding of regional photochemical pollution problems in the East Asian megacity region.

1 Introduction

NO_x ($NO + NO_2$) and volatile organic compounds (VOCs) are two important precursors that drive HO_x radical cycles (Levy, 1971). In the presence of NO_x, VOC oxidation

processes recycle OH and produce photochemical oxidation products such as ozone and oxygenated VOCs (OVOCs). This reaction cycle is highly nonlinear. For example, excess NO_2 may expedite nitric acid formation (Reaction R1), limiting ozone production. In the same context, excess VOCs may expedite peroxy radical production (Reaction R2), which limits OH regeneration from peroxy radicals.

$$OH + NO_2 + M \rightarrow HNO_3 + M \qquad (R1)$$

$$HO_2 + RO_2 \rightarrow ROOH \qquad (R2)$$

The nonlinearity in tropospheric photochemistry has been relatively well studied in the urban regions of developed countries and applied in ozone reduction policy. The Los Angeles metropolitan area has accomplished significant ozone reduction by implementing aggressive emission reductions of both NO_x and VOC, especially from mobile sources (Ryerson et al., 2013). The remarkable ozone abatement was possible due to the fact that there is no significant pollution transport from other metropolitan areas and no significant natural emission sources, especially volatile organic compounds from vegetation (BVOCs; biogenic volatile organic compounds), compared with anthropogenic VOC mostly from mobile sources (Pollack et al., 2013; Huang et al., 2013). In the late 1980s, Trainer et al. (1987) first demonstrated the importance of isoprene (C_5H_8) as a peroxy radical source that can contribute significant ozone production in rural areas. The importance of isoprene in ozone production in urban areas has also been highlighted, e.g., in the Atlanta metropolitan area (Chameides et al., 1988).

Isoprene is a hemiterpenoid species and is the globally dominant VOC emission from vegetation (Arneth et al., 2011; Guenther, 2013). Arguably, isoprene is the most frequently studied BVOC from the perspective of atmospheric oxidation processes and their implications for ozone and aerosol formation. However, significant uncertainty hinders assessing the roles of isoprene in regional and global photochemistry in three fronts. First, there is still significant uncertainty in estimating emission rates from each individual plant species on regional scales (Guenther, 2013). Second, limited isoprene intercomparison results (Barket et al., 2001) suggest that there are large systematic biases among different analytical techniques. Lastly, recent laboratory, theoretical, and field observations suggest significant uncertainty in tropospheric isoprene oxidation processes initiated by OH. Until early 2000, it was thought that three first-generation isoprene oxidation products (methyl vinyl ketone, methacrolein, and formaldehyde) from OH oxidation were enough to constrain isoprene tropospheric oxidation processes for modeling purposes (e.g., Spaulding et al., 2003; Dreyfus et al., 2002). This is an interesting evolution of thoughts considering that Paulson and Seinfeld (1992), one of the pioneering works describing isoprene oxidation, clearly claimed that

22 % of first-generation isoprene oxidation products from the reaction with OH was not identified and likely included multifunctional C5 compounds. Recent advances in analytical techniques (Kim et al., 2013a) have shown that indeed significant C5-hydroxy-carbonyl (e.g., isoprene hydroperoxyaldehydes, HPALD) and peroxide compounds are produced as first-generation isoprene oxidation products (Crounse et al., 2011; Paulot et al., 2009; Wolfe et al., 2012; Zhao and Zhang, 2004). The product yields appeared to be a strong function of NO concentrations (Peeters and Muller, 2010). In general, at low to intermediate NO levels ($\sim$ 100 pptv or lower), the yields of C5-hydroxy-carbonyl compounds become higher. These new findings in the isoprene oxidation process are also closely related to recent findings in unexpectedly high OH concentrations (Hofzumahaus et al., 2009; Lelieveld et al., 2008) and substantial missing OH sinks also known as unexpectedly high OH reactivity in high isoprene environments (Di Carlo et al., 2004; Edwards et al., 2013; Kim et al., 2011; Lou et al., 2010).

These new findings have significant implications for regional air quality especially regarding photochemical ozone and secondary organic aerosols (SOA) production. Despite the strong anthropogenic pollutant emissions in East Asia (China, Japan, and South Korea), recent research has shown that isoprene accounts for a major OH chemical sink in suburban areas near Beijing (Ran et al., 2011), the Pearl River Delta region (Lu et al., 2012), Taipei (Chang et al., 2014), and Seoul (Kim et al., 2013b; Kim et al., 2013). Consequently, modeling studies also clearly show that isoprene contributes significantly to ozone formation in Asian megacity regions. Kim et al. (2013) reported that simulated ozone levels with isoprene chemistry are up to 30 % higher than ozone simulation without isoprene chemistry using the WRF-Chem model, indicating an urgent need to implement improved isoprene chemistry schemes in these models in order to simulate the unexpected higher levels of OH in isoprene-rich environments. This could become an especially serious issue as Hofzumahaus et al. (2009) reported significantly higher-than-expected ($\sim$ 2.6 times at noon) OH levels in the Pearl River Delta region in China. Therefore, the current assessments based on the conventional OH photochemistry could significantly misdiagnose regional air-quality status and mislead policy implementation to reduce photochemical air pollution in the East Asian region. Furthermore, as the importance of BVOC in regional air-quality issues in ozone and SOA formation has been also highlighted in Europe and North America, the uncertainty in isoprene photochemistry has significant implications in urban and suburban air quality in general (Y. Zhang et al., 2008; Sartelet et al., 2012). It should be also noted that HONO has been observed at high levels in the East Asian region even in the daytime ($\sim$ hundreds ppt; Song et al., 2009; Hao et al., 2006; Li et al., 2012). The data analysis has consistently indicated that well-known HONO sources cannot account for the observed level. There-

fore, the implications of HONO as a radical source should also be comprehensively addressed.

We present atmospheric observations of NO_x, CO, VOCs, ozone, and HONO in the Taehwa research forest (TRF) in the Seoul metropolitan area (SMA), South Korea. We use observed data from June 2013 to conduct observationally constrained box-model (UWCM) calculations to estimate OH, HO_2, and RO_2 concentrations with different sets of observational parameters. We discuss current uncertainty in OH-isoprene photochemistry with perspectives of constraining photochemical ozone production and OVOCs precursors of secondary organic aerosols in addition to the roles of unconstrained HONO sources in radical distributions.

2 Methods

The TRF is located ~ 35 km from the center of Seoul, South Korea. The TRF is located at the southeastern edge of the SMA (population of ~ 23 million). TRF has a sampling tower located in the middle of a coniferous tree plantation (200 m by 200 m) with a canopy height of 18 m (*Pinus koraiensis*), surrounded by a deciduous forest mostly composed by oak. The TRF instrumentation has previously been described by Kim et al. (2013) along with the previous trace gas observational results. Therefore, just brief descriptions of analytical techniques are given in this paper.

2.1 CO, NO_x, SO_2, ozone, VOCs, and meteorological parameters

Thermo Fisher Scientific enhanced trace level-gas analyzers are used for CO, NO_x, SO_2, and ozone observations as summarized Table 1. A molybdenum (Mo) converter is used to convert NO_2 to NO for the NO_x analyzer. Although Mo converters are still widely used for NO_2 observations, some of thermally unstable oxygenated reactive nitrogen compounds, especially peroxyacyl nitrates, could be also converted to NO_2 by a Mo converter (Villena et al., 2012). VOC observations are conducted by a high-sensitivity proton transfer reaction mass spectrometer (PTR-MS, Ionicon GmbH). The atmospheric application of this technique is thoroughly reviewed by de Gouw and Warneke (2007). In addition, the instrument suite at TRF is thoroughly described in Kim et al. (2013). PTR-MS can quantify atmospheric VOCs that have higher proton affinity than the proton affinity of H_2O (691 kJ mol^{-1}). Most alkanes have lower proton affinity than water, but alkene, aromatic, and some OVOCs have higher proton affinity and are suitable for quantification using PTR-MS (Blake et al., 2009). These compounds are more reactive than alkane compounds so PTR-MS has the capability to observe reactive atmospheric compounds. The TRF PTR-MS system was set to measure acetaldehyde, acetone, acetic acid, isoprene, methyl vinyl ketone (MVK) + methacrolein (MACR), methyl ethyl ketone (MEK), benzene, xylene (*p*,

m, and *o*), and monoterpenes (MT). Each compound was set to be monitored for 1 s each, resulting in a sample cycle of 15 s. Lower detection limits for the observed VOCs are estimated to be 20 ppt for a 5 s integration with sensitivity of 70 counts ppb^{-1} (2σ). The uncertainty is estimated as 12 % (2σ) for the same integration time. Meteorological parameters such as temperature and humidity are monitored by LSI LASTEM meteorological sensors. All the presented data are from the 15 m (the canopy height is 18 m) sampling line and meteorological sensors collocated at this height too.

PTR-MS with a quadrupole mass filter has an intrinsic limitation that isobaric compounds are all collectively quantified with the same channel (m/z) with a resolution of unit mass. This limitation particularly becomes an issue for investigating the roles of different isomers of MT and sesquiterpenes (SQTs) in photochemistry. For this reason, we also occasionally collect sorbent cartridge samples to analyze MT and SQT speciation in both ambient air and branch enclosure emissions near the sampling tower. As described in Kim et al. (2013), Tenax GR and Carbotrap 5TD packed sorbent cartridges (Markes Int. Ltd., Llantrisant, UK) were used for sampling. The sampled cartridges were shipped to National Center for Atmospheric Research (NCAR) in Boulder, Colorado, USA, for gas chromatography–mass spectrometer (GC-MS) analysis. An Agilent 7890 GC/5975 C electron impact mass spectrometer (GC-MS/FID) in conjunction with a MARKES Unity1/Ultra thermal desorption system optimized for terpenoid analysis quantifies speciated MT and SQT in the sorbent samples. Cartridge samples are both collected from ambient and branch enclosure air. Ambient samples were collected in the midday to early afternoon with a volume of 6 L. Ozone in the ambient air was removed using a Na_2SO_3 filter. Branch enclosure samples were also collected, mostly in the midday time frame, with a volume of 1 L without an ozone filter as zero air was introduced to the branch enclosure. To explore the diurnal differences in BVOC emissions, branch enclosure samplings were conducted every 2 h for 3 consecutive days in mid-June of 2013. We present these analytical results from GC-MS analysis limited to the qualification purpose to examine MT and SQT speciation.

2.2 HONO quantification

HONO was measured with an ion chromatography (IC) coupled with diffusion scrubber. Air was introduced to the diffusion scrubber (Lab solutions Inc., IL, USA) through a 2 m PFA tubing (1/4″ i.d.) at 1.5 L m^{-1} using a filtered orifice restrictor (F-950, air logic, WI, USA). Air flowing through the diffusion scrubber interfaced with deionized water from which HONO was extracted. 50 μL of solution was injected into the IC system through a PEEK loop (Rheodyne, WA, USA) and six-way valve (EV750-100, Rheodyne, WA, USA). Eluent was a mixture of Na_2CO_3 and $NaHCO_3$ which was pumped by a HPLC pump (DX-100, Dionex, CA, USA) into a guard column (IonPac AG14, Dionex, USA) and then

Table 1. Analytical characteristics of trace gas analyzers at TRF.

Chemical species	Manufacturer and model number	Uncertainty	Lower limit of detection
CO	Thermo Scientific 48i TLE	10 %	40 ppb
NO_x	Thermo Scientific 42i-TL with a Mo converter	15 %	50 ppt
SO_2	Thermo Scientific 43i-TLE	10 %	50 ppt
Ozone	Thermo Scientific 49i	5 %	< 1 ppb

analytical column (IonPac AS14, Dionex, USA). The column effluent passed through a suppressor (ASRS 300, Dionex, CA, USA) and HONO was detected as nitrite ion in the conductivity detector (550, Alltech, IL, USA). The entire measurement processes of sampling, chemical analysis, and data acquisition were controlled by a digital timer and data acquisition software (DSchrom-n, DS science, Korea) from which we obtained two measurements every hour. The system was calibrated using a NO_2^- standard solution (Kanto Chemical Co., Inc., Tokyo, Japan) whenever reagents were replaced. The detection limit was 0.15 ppb, estimated from 3σ of the lowest working standard. Specific analytical characteristics are described in Simon and Dasgupta (1995) and Takeuchi et al. (2004).

2.3 UWCM box model

UWCM 2.1 is an open-source box model coded by MAT-LAB (MathWorks®). The model platform can be downloaded from a website (http://sites.google.com/site/wolfegm/code-archive). The box model is embedded with its own HO_x (OH + RO_2)–RO_x (peroxy radical and alkoxy radical)–NO_x coupling chemical mechanism. UWCM utilizes Master Chemical Mechanism v3.2 (MCM 3.2) (Jenkin et al., 1997; Saunders et al., 2003) for near-explicit VOC photo-oxidation schemes. A more detailed model description can be found in Wolfe and Thornton (2011). To minimize uncertainty from the parameterizations of transport and emission, we constrained relatively long-lived trace gases presented in Fig. 1. This box-modeling technique has been commonly used for examination of OH levels that can be justified by the short chemical lifetime of OH (Kim et al., 2013c, 2014; Mao et al., 2010, 2012). Recently developed isoprene photo-oxidation mechanisms shown in Archibald et al. (2010b) are also incorporated in the model. In addition, Kim et al. (2013c) and Wolfe et al. (2014) applied the model in the identical fashion as used for this study to probe radical distributions using comprehensive observational data sets. This study used the UWCM to simulate the diurnal variations of radical pool (OH + HO_2 + RO_2) distributions as observational parameters such as CO, NO_x, ozone, and VOCs are constrained. To fully account for roles of OVOCs in the box model as radical sources, we simulated 3 consecutive days and presented diurnal variations from the third day. The specific parameters (CO, NO_x, ozone, HONO, and VOCs) constrained by obser-

vations are described in Sect. 2.1 and 2.2 and presented in Fig. 1.

3 Results and discussion

3.1 Observational results

Diurnal averages of observed trace gases (1 to 6 June 2013) are shown in Fig. 1. The TRF observatory is in continuous operation and we choose this 6-day period because a regional high-pressure system caused a stagnant air pollution event in this period. In the center of Seoul (the real-time data available at http://www.airkorea.or.kr), carbon monoxide was observed in the similar levels during the focused period (1 to 6 June 2013). However, the NO_2 level observed in central Seoul was much higher (20–50 ppb) compared to observed levels at TRF. The reason can be attributed to differences between the chemical lifetime of CO ($\sim$ 1 month) and NO_2 ($\sim$ a few hours to 1 day). The observations clearly indicate that the TRF is not directly influenced by fresh SMA pollution plumes although the TRF is very close to the center of Seoul (30 km away from the city center), as a regional modeling study shows most of CO and NO_x sources are located in the city center (Ryu et al., 2013). Similar observations were also reported for other East Asian megacities such as Beijing (Ma et al., 2012), where $\sim$ 30 and 15 ppb of NO_2 were observed at noon in the urban and the adjacent rural sites, respectively. In contrast, there were no noticeable differences in CO levels between the urban and rural sites ($\sim$ 1–2 ppm). The observed CO, NO_x, and SO_2 levels in TRF were much lower than those observed in the suburban regions of Chinese megacities such as Beijing (Ma et al., 2012), Shanghai (Tie et al., 2013), and the Pearl River Delta region (Lu et al., 2012) and similar to the observed levels in Tokyo, Japan (Yoshino et al., 2012).

Previous VOC observations in the SMA consistently have shown that toluene is the dominant anthropogenic VOC followed by other aromatic compounds such as xylene and benzene (Kim et al., 2012; Na and Kim, 2001). Na and Kim (2001) reported high concentrations of propane from household fuel use. However, recent observation results from the photochemical pollution observational network managed by National Institute of Environmental Research of South Korea in the SMA clearly indicate that propane levels have declined and are now much lower than the levels previously
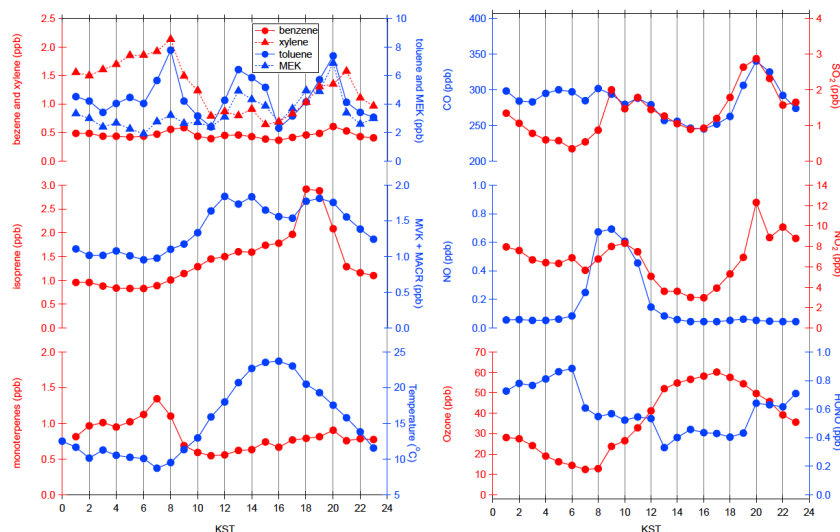
Figure 1. Averaged temporal variations in observed trace gases and ambient temperature at TRF (1 to 6 June 2012; KST stands for Korean standard time, GMT + 9). The uncertainty for each observable is listed in the main text.

observed (NIER, 2010). This is probably caused by the implementation of a policy changing household fuel sources from propane to methane. Kim et al. (2012) presented detailed aromatic VOC distributions in the SMA from four different urban observational sites. On average, observed toluene concentrations were ∼ 7 times higher than the observed levels of xylene and benzene. At the TRF a similar anthropogenic VOC speciation distribution was observed as shown in Fig. 1. The observed toluene and MEK mixing ratios were much higher than benzene and xylene. MEK is detected in m/z of 73^+ by PTR-MS. Although methyl glyoxal, an atmospheric VOC oxidation product, is also detected on the same mass, we assumed that 73^+ of m/z signals are mostly from MEK, an anthropogenic VOC, since the temporal variation follows that of anthropogenic VOC such as toluene and xylene. In addition, atmospheric lifetime of methyl glyoxal is much shorter than MEK.

As the observation facility is located in the middle of a pine tree plantation (*Pinus koraiensis*), MT are consistently observed. The temporal variation of MT is affected by the planetary boundary layer evolution, with a pattern of higher MT levels during night than those of midday as has been often reported in other forest environments (Bryan et al., 2012; Kim et al., 2010). This can be explained by interplays between boundary layer evolution and temperature-dependent MT emission. It should also be noted that the continuous branch enclosure BVOC emission observations indicate that the daily maxima of MT and SQT emissions were observed in the midday (between noon and 2 p.m. local time). The observed MT and SQT speciation information at midday is summarized in Table 2. Table 2a summarizes branch enclosure sample analysis results and ambient sample analysis results are summarized in Table 2b. In general, observed MT

and SQT in the ambient air are consistent with previously observed distributions (Kim et al., 2013). α-pinene and β-pinene were the dominant monoterpene and longifolene was the only detected SQT species. In contrast, the branch enclosure observation results, reflecting BVOC emission, indicate high emission of very reactive MT and SQT species such as β-myrcene, α-caryophyllene, and β-caryophyllene. The fast oxidation of these highly reactive terpenoid species is expected to limit the atmospheric presence of the compounds. Therefore, photochemical oxidation processes of these compounds may have been neglected. Investigating emissions and photochemistry of these reactive terpenoid compounds can constrain potential missing OH reactivity and SOA production from highly oxidized reaction products.

Isoprene is produced from carbon recently fixed through photosynthesis, resulting in higher emissions and atmospheric concentrations during the daytime. The temporal variation shown in Fig. 1 reveals an isoprene concentration maximum between 17:00 and 20:00. In addition, the ratios of MVK + MACR, major isoprene oxidation products and isoprene at this period, are significantly lower than those of late morning to early afternoon. The enhanced isoprene levels in the late afternoon or early evening have been also reported in previous studies (Apel et al., 2002; Bryan et al., 2012). The branch enclosure observations demonstrate that isoprene is not emitted from the pine plantation but rather transported from surrounding broadleaf forests, because right outside of the pine plantation (200 m × 200 m) is a forested area dominated by oak trees. Oak comprises 85 % of broadleaf trees in South Korea (Lim et al., 2011). Lim et al. (2011) quantified isoprene emission rates for five representative oak species in South Korea and report a wide emission range from oaks that are negligible isoprene emitters ($< 0.004\,\mu gC\,dw^{-1}\,h^{-1}$;

**Table 2.** Terpenoid speciation analysis results from GC-MS (a) branch enclosure and (b) ambient air samples.

(a)

Terpenoids	*Composition (%)	Speciation	*Composition (%)
Isoprene	0.5		
Monoterpenes	92.9	α-pinene	36.7
		camphene	13.1
		β-pinene	12.0
		β-myrcene	27.7
		α-terpinolene	1.9
		d-limonene	8.6
Sesquiterpenes	6.6	β-caryophyllene	53.2
		α-caryophyllene	46.8

(b)

Terpenoids	*Composition (%)	Speciation	*Composition (%)
Monoterpenes	98.6	α-pinene	38.8
		β-pinene	36.5
		camphene	13.5
		d-limonene	11
Sesquiterpenes	1.4	longifolene	100

* Composition is calculated based on the mixing ratio scale.

standard emission rates) to others with very high isoprene emission rates of $130\,\mu gC\,dw^{-1}\,h^{-1}$. It is also noticeable that isoprene is observed in high levels (up to 1 ppb) even during the night. Observational results from the Pearl River Delta region in China also show high-isoprene-concentration episodes of more than 1 ppb during the night (Lu et al., 2012). As there are some speculations on potential artifacts on isoprene measurements using PTR-MS in environments with large oil and gas evaporative sources (Yuan et al., 2014), the assessments of the potential artifacts should be investigated further in the Asian megacity region.

Contributions from each trace gas species towards ambient OH reactivity are shown in Fig. 2. This is calculated as the product of the observed species concentration and its rate constant for reaction with OH. Observed OH reactivity from VOCs are much higher than from other trace gases such as CO, NO_x, SO_2, and ozone. Among the observed VOC species, BVOCs such as isoprene, α-pinene, and β-pinene accounted for significantly higher OH reactivity in comparison to the observed aromatic volatile organic compounds such as toluene, benzene, xylene, and MEK. Isoprene accounts for the highest OH reactivity especially during the daytime. This analysis is consistent with reports from other suburban observations from East Asian megacities such as Beijing (Ran et al., 2011) and the Pearl River Delta region (Lou et al., 2010) in China and the Kinki region in Japan (Bao et al., 2010).

HONO levels up to 1 ppb were observed in the early morning and were consistently higher than 0.5 ppb during the daytime. These observed levels are substantially higher than reported observations from forest environments in North America (Ren et al., 2011; Zhou et al., 2011), where NO_x
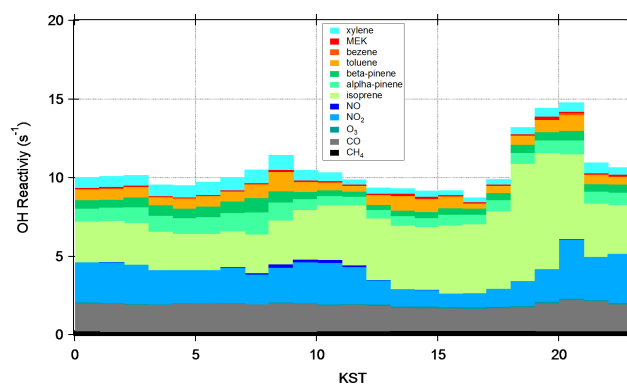
Figure 2. The temporal variations of OH reactivity calculated from the observed data set at TRF (Fig. 1).

(~ 1 ppb) is substantially lower than the level observed at TRF. Ren et al. (2011) reported 30–60 ppt of HONO at the Blodgett Forest research station in the western foothills of the Sierra Nevada in the late summer of 2007. Zhou et al. (2011) also reported the similar levels of HONO (below 100 ppt) from the PROPHET forest, a mixed hardwood forest in northern Michigan (Pellston, MI). However, significantly higher HONO levels (~ 200 ppt to 2 ppb) were reported by Li et al. (2012) from a rural observational site in the Pearl River Delta region near Guangzhou, where comparable NO_2 levels with TRF were observed. The high HONO levels (a few hundred ppt) especially during the daytime have been consistently reported near East Asian megacities such as Beijing (Li et al., 2012), Shanghai (Hao et al., 2006), and Seoul (Song et al., 2009). Still these are limited data sets and further comprehensive analysis, especially more extensive observation, is required. However, recently proposed HONO production mechanisms may be able to explain the higher levels in the East Asian megacity region. One is HONO production from NO_2 photo-excitation (Wong et al., 2012) as the region usually has high NO_2 concentrations. Zhou et al. (2011) claimed that significant HONO could be generated from nitrate photolysis processes on forest canopy surface by presenting observational data from a hardwood forest in Pellston, MI. Finally, HONO emission from soil bacteria is also proposed (Oswald et al., 2013). Oswald et al. (2013) found differences as much as 2 orders of magnitude in HONO emissions from soil samples from different environments (e.g., pH and nutrient contents). In addition, as most of observations in the East Asia regions were conducted with ion-chromatography-based methods, more direct HONO quantification techniques such as a chemical ionization mass spectrometry technique (Roberts et al., 2010) need to be used to characterize any potential interferences such a high NO_x environment (e.g., N_2O_5).

Table 3. A summary of critical differences in input parameters for four different model simulation scenarios presented in this study. The isoprene chemical scheme is based on Archibald et al. (2010a).

	HPALD chemistry	Observational constraints
Scenario I	No	[c]All
Scenario II	[a]Peeters and Muller (2010)	[c]All
Scenario III	[b]Crounse et al. (2011)	[c]All
Scenario IV	No	[c]All but HONO

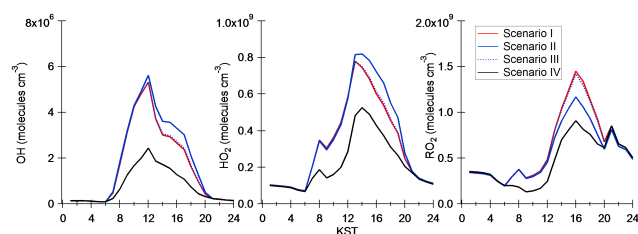[a] k298 = ∼0.08 for isoprene peroxy radical isomerization rate that produces HPALD;
[b] k298 = 0.002 for isoprene peroxy radical isomerization rate; [c] all the observed diurnal variations that appeared in Fig. 1 are constrained in the model along with ambient pressure and humidity.

Figure 3. The temporal variations of OH (left panel), HO_2 (middle panel), and RO_2 (right panel) calculated by four different observationally constrained UWCM box-model scenarios.

3.2 HO_x model calculations to examine different isoprene photo-oxidation scenarios and the roles of unconstrained HONO sources

The presented observational results are used to constrain the UWCM box model. We evaluate uncertainties in the tropospheric oxidation capacity and how it affects our ability to constrain ozone and OVOCs production. The observational results clearly indicate that isoprene is the most dominant OH sink among the observed VOCs. In addition, NO concentrations were higher in the 600 to 800 ppt range in the morning. However, afternoon levels were substantially lower in the 50 to 100 ppt range. The environment provides a unique opportunity to examine implications of isoprene photochemistry in various NO conditions.

We conducted model simulation under four different scenarios. Each scenario is described in Table 3. The quantitative assessments of the impacts on radical concentrations (OH, HO_2, and RO_2) from unknown HONO sources are evaluated by examining the outcomes of the model simulations with and without observed HONO. To evaluate the impacts of HPALD photolysis and isoprene peroxy radical recycling in the radical pool, each chemical mechanism is selectively constrained by different scenarios. For HPALD chemistry, we adapted two different HPALD formation rate constants published by Peeters and Muller (2010) and Crounse et al. (2011). The formation rates from Peeters and Muller (2010) are about 40 times faster than those from Crounse et al. (2011) in 298 K. Although there have been speculations about other radical recycling mechanisms such as peroxy –peroxy radical reactions (Lelieveld et al., 2008) and unknown reducing agents showing similar chemical behaviors as NO (Hofzumahaus et al., 2009), we do not evaluate these possibilities as there are no specific chemical mechanisms.

Modeled OH, HO_2, and RO_2 from the four different model scenarios are shown in Fig. 3. A summary of averaged OH, HO_2, and RO_2 concentrations in the morning (08:00–11:00) and the afternoon (13:00–16:00) from each simulation is shown in Table 4. With respect to the base run results (Scenario I), Scenario III with the lower HPALD formation rate does not cause noticeable differences in radical con-

centrations. Adapting higher HPALD formation rates (Scenario II) causes significant differences in radical distribution especially in RO_2. This difference is likely caused by the fact that significant isoprene peroxy radical is converted to HPALD. The higher levels of discrepancy are found in RO_2 between Scenario I and Scenario II in the afternoon when low NO concentrations are observed, which efficiently facilitates HPALD formation. Similarly, a larger OH discrepancy ($\sim 20\%$) between Scenario I and Scenario II is observed in the afternoon.

Striking differences can be found in the model simulation results with or without constraining observed HONO as shown in Fig. 3. Model calculation results from Scenario IV indicate significantly smaller OH, HO_2, and RO_2 concentrations than the concentrations calculated from the counter part (Scenario I), which contains identical constraints and isoprene photochemistry except constraining observed HONO. Again, this clearly indicates that more thorough evaluations of the impacts of HONO on air quality are needed to precisely constrain photochemical processes in the region along with evaluations of the currently available analytical techniques as argued in Sect. 3.1.

3.3 Implications of the uncertainty in HO_x estimations in assessing photochemical ozone and OVOC production

Two competing chemical reactions (R3 vs. R4, R5, R6) determine radical distribution regimes.

$$RO_2 + NO \rightarrow RO + NO_2 \tag{R3}$$

$$RO_2 + HO_2 \rightarrow ROOH + O_2 \tag{R4}$$

$$RO_2 + RO_2 \rightarrow ROOR + O_2 \tag{R5}$$

$$HO_2 + HO_2 \rightarrow H_2O_2 + O_2 \tag{R6}$$

When the rate of Reaction (R3) gets much faster than the sum of reaction rates of Reactions (R4), (R5), and (R6), then

Table 4. A summary of radical distributions from the observationally constrained box-model simulation results.

Local time	OH		HO$_2$		RO$_2$		Constraints
	08:00–12:00	13:00–16:00	08:00–12:00	13:00–16:00	08:00–12:00	13:00–16:00	
Scenario I	3.85×10^6	3.08×10^6	4.10×10^8	7.02×10^8	3.65×10^8	1.14×10^9	All
Scenario II	3.99×10^6	3.69×10^6	3.99×10^8	7.86×10^8	3.51×10^8	9.62×10^8	All
Scenario III	3.86×10^6	3.13×10^6	4.09×10^8	7.09×10^8	3.64×10^8	1.12×10^9	All
Scenario IV	1.61×10^6	1.61×10^6	1.95×10^8	4.82×10^8	1.75×10^8	7.25×10^8	All but HONO

unit: molecules cm^{-3}

radical recycling processes become more efficient than radical destruction processes. In this radical recycling regime, OH, a universal tropospheric oxidant, is well buffered to maintain the elevated OH levels. However, the radical destruction regime can be defined when the radical recycling rates (Reaction R3) are slower than the radical destruction reaction rates (Reactions R4 + R5 + R6). Although some recent field studies (e.g., Lelieveld et al., 2008) suggest that we may need to reconsider R4 as a radical recycling process rather than a radical destruction process, in this study we follow the conventional classification of radical chemistry regimes since recent laboratory characterizations have shown that OH recycling from the RO$_2$ + HO$_2$ reaction should be insignificant (Liu et al., 2013; Villena et al., 2012; Fuchs et al., 2013). The temporal variations of radical–radical reaction rates from the model simulation scenarios are shown in Fig. 4. In general, the radical reaction rates are as much as doubled once observed HONO is constrained in the model calculations (e.g., Scenario IV). This is because unaccounted HONO in the model calculations causes significant underestimations in the radical pool (OH + HO$_2$ + RO$_2$) size with respect to the constrained HONO scenarios as shown in Fig. 4. In addition, in the afternoon when NO concentration becomes lower, the RO$_2$ + HO$_2$ reaction rates get close or slightly higher than those of RO$_2$ + NO in the afternoon for the all model scenarios, constrained by observed HONO. This is surprising, as the radical destruction regime is usually associated with low NO$_x$ conditions. Suburban regions of megacities including the TRF in general show high NO$_x$ conditions. However, radical recycling rates are determined by concentrations of NO. The fraction of NO in the NO$_x$ pool is determined by competing reactions between NO$_2$ photolysis and oxidation reactions of NO by ozone, HO$_2$, and RO$_2$ radicals. Once we assume the pseudo-steady state of NO, then NO in the NO$_x$ pool (Leighton, 1961) can be expressed as

$$[NO] = J_{NO_2}[NO_2] / \left(k_{NO+O_3}[O_3] + k_{NO+HO_2}[HO_2] \right.$$
$$\left. + k_{NO+RO_2}.[RO_2] \right) \qquad (1)$$

This mathematical expression clearly shows that NO levels are dependent on NO$_x$ mostly composed of NO$_2$. At
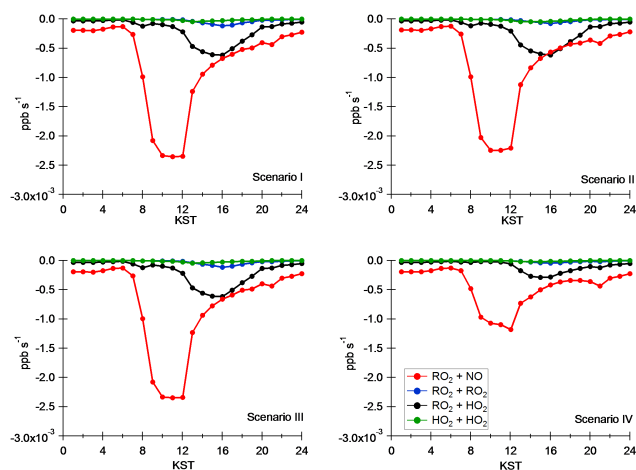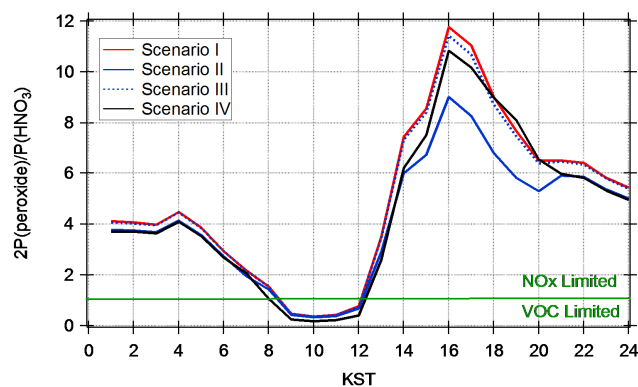

Figure 4. The temporal variations of radical recycling (red) and destruction (blue, black, and green) rates calculated using the UWCM box model for different model scenarios.

the same time, the fraction of NO in NO$_x$ is anti-correlated with ozone, HO$_2$, and RO$_2$ concentrations. Therefore, the size of the radical pool composed of HO$_2$ and RO$_2$ is relevant for determining the fractions of NO in given NO$_x$ levels. High HO$_2$ and RO$_2$ are likely observed in high-VOC regions such as forested areas. This could cause a smaller fraction of NO in the given NO$_x$ pool so radical recycling gets relatively weaker compared with radical destruction reaction pathways. More quantitative approaches are required to categorize radical reaction pathways rather than qualitative categorization such as high or low NO$_x$ regimes. One should keep in mind that the pseudo-steady-state assumption requires precise NO$_2$ quantification, which may not be the case in our study as the Mo converter used for the NO$_2$ quantification could have interferences (Table 1). The overestimation due to thermal dissociations of reactive oxygenated nitrogen species has been reported to be 20 to 83 % (Ge et al., 2013; Steinbacher et al., 2007). In addition, Mannschreck et al. (2004) presented the NO–NO$_2$–ozone photostationary state analysis using a 4-year data set from a rural observational site in Hohenpeissenberg, Germany. The results indicate that the pseudo-steady-state assumption considering only NO–NO$_2$–ozone deviates about a factor of 2 from the

stationary state on average. Even with the consideration of peroxy radical chemistry, the pseudo-steady-state assumption is only valid for 13–32 % of the observational period. The authors speculated that local NO_2 sources, local NO or ozone sinks, or rapid changes in J_{NO_2} and ozone can break the pseudo-steady state. Nonetheless, the argument that NO is a more critical parameter in determining radical distributions than NO_x levels still holds.

Conventionally, efficient ozone production can be achieved by the balance between nitric acid production rates (P_{HNO_3}, $OH + NO_2$) and peroxide production rates (P_{ROOH}, $HO_2 + RO_2$, or $P_{H_2O_2}$ $HO_2 + HO_2$) (Sillman and He, 2002). The imbalance will cause ozone production sensitivity towards either NO_x or VOCs. A comprehensive photochemical model analysis (Tonnesen and Dennis, 2000a, b) demonstrated that in a wider range of ozone concentrations, the VOC and NO_x limited regimes can be determined by the ratios of $P_{H_2O_2}$ and P_{HNO_3}. Kleinman (2000) and Sillman and He (2002) presented an observation-based ozone production regime evaluation method comparing peroxide production rates (P(peroxide)) and nitric acid production rates (P(HNO$_3$)). A series of modeling studies have been conducted to characterize ozone production regimes in the suburban regions of East Asian megacities and have consistently concluded that the role of isoprene is important in ozone production. However, most of these studies have concluded that East Asian megacity regions are mostly in the VOC limited regime (Tseng et al., 2009; Y. H. Zhang et al., 2008; Lim et al., 2011; Cheng et al., 2010; Shao et al., 2009a, b; Xing et al., 2011). Recently, however, a modeling study by Li et al. (2013) in the Pearl River Delta region in China demonstrated the time dependence of ozone production regimes. Specifically, with high NO_x emissions in the morning the regional ozone production regime is categorized as VOC limited. In contrast, in the afternoon when the highest ozone concentrations are observed, a NO_x-limited regime is often found. In addition, a box-modeling study constrained by observation on top of Mount Tai in central east China also reported a NO_x-limited ozone production regime (Kanaya et al., 2009). The obvious issue to be addressed is that all of the above studies neglected how the uncertainty in hydroxyl radical chemistry would affect the ozone production regime. Moreover, HONO has been rarely constrained by observations in the previous modeling studies. Figure 5 shows the temporal variations of $2P$(peroxide) / P(HNO$_3$) from all four different model scenarios. As shown in the figure, the ratio above 1 indicates the NO_x limited regime and the VOC limited regime can be determined when the ratio is below 1. The NO_x limited ozone formation regime occurred on most days except in the morning, when high NO_x levels were observed regardless of the HO_x simulation scenarios. This is consistent with the recent modeling study for the Pearl River Delta region by Li et al. (2013). Differences among the scenarios are not noticeable in the morning when NO is high but noticeable

Figure 5. The temporal variations of $P_{H_2O_2}$ / P_{HNO_3} calculated from the UWCM box model from four different model scenarios.

differences can be found in the afternoon, which may cause uncertainty in assessing the optimal level of NO_x and VOC emission controls from a policy perspective. In general, the model calculation results with faster HPALD formation rates indicate lower $2P$(peroxide) / P(HNO$_3$) in the afternoon. This analysis indicates that it is difficult to determine an effective policy implementation for NO_x or VOC controls to achieve ozone abatement around Asian megacities where isoprene is a significant OH sink without accurate understanding of radical-isoprene interactions (e.g., Kim et al., 2013b). Again, it should be noted the possibility of systematic NO_2 overestimations from the Mo converter use as discussed. The overestimation will directly translate into overestimated P(HNO$_3$). Therefore, it is likely that the ozone production regime at TRF is shifted towards the NO_x limited regime in reality.

Another unresolved uncertainty in understanding tropospheric OH is its chemical loss rates. The limited observations of OH reactivity in BVOC dominant environments show consistent unaccounted OH chemical loss with observational data sets (Di Carlo et al., 2004; Edwards et al., 2013; Kim et al., 2011; Lou et al., 2010; Nölscher et al., 2012; Nakashima et al., 2014; Sinha et al., 2010). Two different processes are speculated to cause unaccounted OH loss known as missing OH reactivity: (1) primary emissions of unmeasured or unknown compounds and (2) oxidation products of well-known BVOCs, especially isoprene. Most studies conducted in coniferous forests where monoterpenes are dominant primary BVOC emissions have concluded that unmeasured or unknown primary BVOC emissions caused missing OH reactivity (Sinha et al., 2010; Nakashima et al., 2014). Nonetheless, studies conducted in isoprene dominant environments in mostly broadleaf or mixed forests have concluded that the main cause of missing OH reactivity is the oxidation products of isoprene (Edwards et al., 2013; Kim et al., 2011). Edwards et al. (2013) presented a thorough analysis on potential impacts of isoprene oxidation products that are not routinely constrained by observations. The authors found
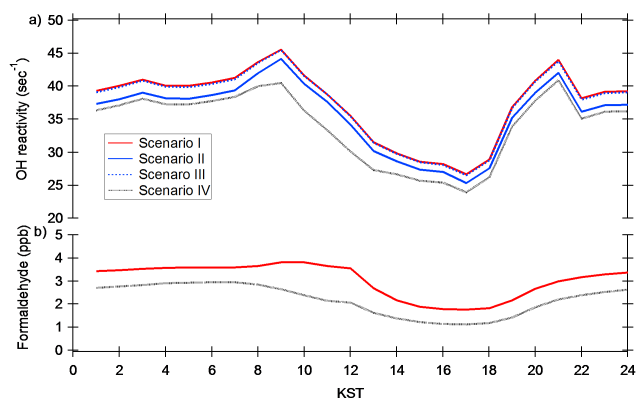
Figure 6. The temporal distributions of UWCM-calculated OH reactivity **(a)** and formaldehyde **(b)** from different model calculation scenarios.

significant contributions from secondary oxidation products such as multi-functional oxygenated compounds.

Figure 6a shows the temporal variations of total OH reactivity calculated from five different model scenarios (I through IV). The highest and the lowest OH reactivity levels were predicted from model calculations of Scenario I and Scenario IV, respectively. This observation is directly correlated with calculated RO_2 levels as the lowest and highest RO_2 levels were calculated from Scenario I and Scenario IV, respectively. Since VOC precursors and trace gases were all constrained by observations in the model calculations, the differences in model-calculated OH reactivity should be mainly caused by the oxidation products of VOCs. This can be confirmed by the comparisons of model-calculated formaldehyde concentrations from Scenario I and IV as formaldehyde is a dominant oxidation product of isoprene (Fig. 6b). The differences in formaldehyde levels suggest differences in OH reactivity levels from OVOCs in each model simulation. In summary, uncertainty in radical distributions especially RO_2 levels is directly propagated into uncertainty in OVOC formation.

These calculated results provide an upper limit of potential contributions from the oxidation products of the constrained VOC precursors considering that the box model does not consider dry-deposition processes; Karl et al. (2010) and Edwards et al. (2013) suggested that there is significant uncertainty associated with the parameterizations of dry deposition especially OVOCs. Still, this analysis suggests that significant missing OH reactivity can be found without constraining OVOCs. OVOCs, especially multi-functional highly oxidized compounds, are precursors for SOA. Therefore, uncertainty surrounding missing OH reactivity significantly undermines our ability to constrain SOA formation and aerosol growth.

4   Summary and conclusions

We presented trace gas observation results from the TRF near the center of Seoul, South Korea. The data set provides important constraints to evaluate the HO_x pool at the site where both anthropogenic and biogenic influences become important factors in determining oxidation capacity. Although the site is in the vicinity of a megacity with 25 million people, isoprene accounted for most of the OH loss from observed atmospheric hydrocarbon species during the 6-day focus period in early June 2013 during a regional pollution episode. In addition, observed NO_x levels were substantially lower than observed values in the center of the SMA. These observations indicate that impacts of megacity pollution on suburban BVOC photochemistry can be observed at the TRF.

Four different model scenarios are employed to investigate the radical (OH, HO_2, and RO_2) distributions using the UWCM box model. The observed trace gas data were constrained and the photochemical mechanisms (MCM 3.2) of seven VOC species with high levels at the TRF were integrated. The uncertainty in isoprene peroxy radical chemistry results in a wider range of OH, HO_2, and RO_2 distributions. Unconstrained HONO sources also cause a quite high level of underestimation in a radical pool (OH + HO_2 + RO_2). OH simulation from the different model scenarios indicates much larger discrepancies (up to 3 times) than simulations for HO_2 and RO_2 (up to twofold). OH is simulated in higher levels with the consideration of an additional OH recycling channel from fast HPALD formation chemistry (Peeters and Muller 2010). However, the RO_2 simulations result in lower levels as HPALD formation depletes the RO_2 pool, which mostly composed of isoprene peroxy radicals. These results suggest that direct HO_2 and RO_2 observations can provide pivotal information about radical recycling and isoprene peroxy radical chemistry (Kim et al., 2013c; Wolfe et al., 2014). More studies on characterizing existing techniques to quantify HO_2 (Fuchs et al., 2011) and developing new techniques (Horstjann et al., 2014) are needed. In addition, the simulations with recently developed isoprene photo-oxidation chemistry show that radical termination processes (e.g., peroxide formation) get more efficient than radical recycling processes in the afternoon. This may come as a surprise as in general we expect the high NO_x conditions in the suburban regions of a megacity to have effective radical recycling. However, the critical factor determining competing reaction channels of recycling and peroxide formation is NO concentrations. Ratios of NO to NO_2 are not only correlated with NO_2 concentrations and photolysis constants but also anti-correlated with RO_2, HO_2 and ozone concentrations and relevant kinetic constants as shown in (Eq. 1). Therefore, a semi-quantitative term such as the high "NO_x" regime is not a proper term to define radical recycle regimes especially in high radical environments (e.g., HO_2 and RO_2) such as forest environments.

These uncertainties in estimating the radical pool size and distribution directly affect our ability to constrain photochemical ozone and OVOC production. The nonlinear response of ozone production to NO_x and VOC abundances are determined by OH, HO_2, RO_2, and NO_2 concentrations. Regardless of which model calculation scenario we adapt, the TRF photochemical state appears to be a NO_x-limited ozone production regime, except in the morning when the VOC limited regime is observed. A noticeable range of NO_x sensitivity was calculated from the four different model scenarios, especially in the afternoon. These analysis results, therefore, suggest that an accurate scientific understanding of isoprene-OH interactions should form the basis for an effective policy implementation to reduce photochemical pollution in the suburbs of Seoul and similar East Asian megacities. In addition, OVOC production is predicted to significantly vary depending on the model simulation scenarios. The fate of these OVOCs is uncertain and can include deposition, photolysis, or condensation. Our limited understanding of OVOCs contributes substantially to the overall uncertainty in radical photochemistry and should be addressed by studies that quantify the processes controlling OVOC production and loss.

Edited by: K. Schaefer

References

Apel, E. C., Riemer, D. D., Hills, A., Baugh, W., Orlando, J., Faloona, I., Tan, D., Brune, W., Lamb, B., Westberg, H., Carroll, M. A., Thornberry, T., and Geron, C. D.: Measurement and interpretation of isoprene fluxes and isoprene, methacrolein, and methyl vinyl ketone mixing ratios at the PROPHET site during the 1998 Intensive, J. Geophys. Res.-Atmos., 107, 4034, doi:10.1029/2000jd000225, 2002.

Archibald, A. T., Cooke, M. C., Utembe, S. R., Shallcross, D. E., Derwent, R. G., and Jenkin, M. E.: Impacts of mechanistic changes on HO_x formation and recycling in the oxidation of isoprene, Atmos. Chem. Phys., 10, 8097–8118, doi:10.5194/acp-10-8097-2010, 2010a.

Archibald, A. T., Jenkin, M. E., and Shallcross, D. E.: An isoprene mechanism intercomparison, Atmos. Environ., 44, 5356–5364, doi:10.1016/J.Atmosenv.2009.09.016, 2010b.

Arneth, A., Schurgers, G., Lathiere, J., Duhl, T., Beerling, D. J., Hewitt, C. N., Martin, M., and Guenther, A.: Global terrestrial isoprene emission models: sensitivity to variability in climate and vegetation, Atmos. Chem. Phys., 11, 8037–8052, doi:10.5194/acp-11-8037-2011, 2011.

Bao, H., Shrestha, K. L., Kondo, A., Kaga, A., and Inoue, Y.: Modeling the influence of biogenic volatile organic compound emissions on ozone concentration during summer season in the Kinki region of Japan, Atmos. Environ., 44, 421–431, doi:10.1016/J.Atmosenv.2009.10.021, 2010.

Barket, D. J., Hurst, J. M., Couch, T. L., Colorado, A., Shepson, P. B., Riemer, D. D., Hills, A. J., Apel, E. C., Hafer, R., Lamb, B. K., Westberg, H. H., Farmer, C. T., Stabenau, E. R., and Zika, R. G.: Intercomparison of automated methodologies for determination of ambient isoprene during the PROPHET 1998 summer campaign, J. Geophys. Res.-Atmos., 106, 24301–24313, doi:10.1029/2000jd900562, 2001.

Blake, R. S., Monks, P. S., and Ellis, A. M.: Proton-Transfer Reaction Mass Spectrometry, Chem. Rev., 109, 861–896, 2009.

Bryan, A. M., Bertman, S. B., Carroll, M. A., Dusanter, S., Edwards, G. D., Forkel, R., Griffith, S., Guenther, A. B., Hansen, R. F., Helmig, D., Jobson, B. T., Keutsch, F. N., Lefer, B. L., Pressley, S. N., Shepson, P. B., Stevens, P. S., and Steiner, A. L.: In-canopy gas-phase chemistry during CABINEX 2009: sensitivity of a 1-D canopy model to vertical mixing and isoprene chemistry, Atmos. Chem. Phys., 12, 8829–8849, doi:10.5194/acp-12-8829-2012, 2012.

Chameides, W. L., Lindsay, R. W., Richardson, J., and Kiang, C. S.: The Role of Biogenic Hydrocarbons in Urban Photochemical Smog – Atlanta as a Case-Study, Science, 241, 1473–1475, 1988.

Chang, C. C., Wang, J. L., Leung, S.-C. C., Chang, C. Y., Lee, P.-J., Chew, C., Liao, W.-N., and Ou-Yang, C.-F.: Seosonal characteristics of biogenic and anthropogenic isoprene in tropical-subtropical urban environments, Atmos. Environ., 99, 298–308, 2014.

Cheng, H. R., Guo, H., Saunders, S. M., Lam, S. H. M., Jiang, F., Wang, X. M., Simpson, I. J., Blake, D. R., Louie, P. K. K., and Wang, T. J.: Assessing photochemical ozone formation in the Pearl River Delta with a photochemical trajectory model, Atmos. Environ., 44, 4199–4208, doi:10.1016/J.Atmosenv.2010.07.019, 2010.

Crounse, J. D., Paulot, F., Kjaergaard, H. G., and Wennberg, P. O.: Peroxy radical isomerization in the oxidation of isoprene, Phys. Chem. Chem. Phys., 13, 13607–13613, doi:10.1039/C1cp21330j, 2011.

de Gouw, J. and Warneke, C.: Measurements of volatile organic compounds in the earths atmosphere using proton-transfer-reaction mass spectrometry, Mass Spectrom. Rev., 26, 223–257, 2007.

Di Carlo, P., Brune, W. H., Martinez, M., Harder, H., Lesher, R., Ren, X. R., Thornberry, T., Carroll, M. A., Young, V., Shepson, P. B., Riemer, D., Apel, E., and Campbell, C.: Missing OH reactivity in a forest: Evidence for unknown reactive biogenic VOCs, Science, 304, 722–725, doi:10.1126/Science.1094392, 2004.

Dreyfus, G. B., Schade, G. W., and Goldstein, A. H.: Observational constraints on the contribution of isoprene oxidation to ozone production on the western slope of the Sierra Nevada, California, J. Geophys. Res.-Atmos., 107, 4365, doi:10.1029/2001jd001490, 2002.

Edwards, P. M., Evans, M. J., Furneaux, K. L., Hopkins, J., Ingham, T., Jones, C., Lee, J. D., Lewis, A. C., Moller, S. J., Stone, D., Whalley, L. K., and Heard, D. E.: OH reactivity in a South East Asian tropical rainforest during the Oxidant and Particle Photochemical Processes (OP3) project, Atmos. Chem. Phys., 13, 9497–9514, doi:10.5194/acp-13-9497-2013, 2013.

Fuchs, H., Bohn, B., Hofzumahaus, A., Holland, F., Lu, K. D., Nehr, S., Rohrer, F., and Wahner, A.: Detection of HO_2 by laser-induced fluorescence: calibration and interferences from RO_2 radicals, Atmos. Meas. Tech., 4, 1209–1225, doi:10.5194/amt-4-1209-2011, 2011.

Fuchs, H., Hofzumahaus, A., Rohrer, F., Bohn, B., Brauers, T., Dorn, H. P., Haseler, R., Holland, F., Kaminski, M., Li, X., Lu, K., Nehr, S., Tillmann, R., Wegener, R., and Wahner, A.: Experimental evidence for efficient hydroxyl radical regeneration in isoprene oxidation, Nat. Geosci., 6, 1023–1026, doi:10.1038/Ngeo1964, 2013.

Ge, B. Z., Sun, Y. L., Liu, Y., Dong, H. B., Ji, D. S., Jiang, Q., Li, J., and Wang, Z. F.: Nitrogen dioxide measurement by cavity attenuated phase shift spectroscopy (CAPS) and implications in ozone production efficiency and nitrate formation in Beijing, China, J. Geophys. Res.-Atmos., 118, 9499–9509, doi:10.1002/Jgrd.50757, 2013.

Guenther, A.: Biological and chemical diversity of biogenic volatile organic emissions into the atmosphere, Atmos. Sci., 2013, 786290, doi:10.1155/2013/786290, 2013.

Hao, N., Zhou, B., Chen, D., and Chen, L. M.: Observations of nitrous acid and its relative humidity dependence in Shanghai, J. Environ. Sci.-China, 18, 910–915, doi:10.1016/S1001-0742(06)60013-2, 2006.

Hofzumahaus, A., Rohrer, F., Lu, K. D., Bohn, B., Brauers, T., Chang, C. C., Fuchs, H., Holland, F., Kita, K., Kondo, Y., Li, X., Lou, S. R., Shao, M., Zeng, L. M., Wahner, A., and Zhang, Y. H.: Amplified Trace Gas Removal in the Troposphere, Science, 324, 1702–1704, doi:10.1126/science.1164566, 2009.

Horstjann, M., Andrés Hernández, M. D., Nenakhov, V., Chrobry, A., and Burrows, J. P.: Peroxy radical detection for airborne atmospheric measurements using absorption spectroscopy of NO_2, Atmos. Meas. Tech., 7, 1245–1257, doi:10.5194/amt-7-1245-2014, 2014.

Huang, M., Bowman, K. W., Carmichael, G. R., Pierce, R. B., Worden, H. M., Luo, M., Cooper, O. R., Pollack, I. B., Ryerson, T. B., and Brown, S. S.: Impact of Southern California anthropogenic emissions on ozone pollution in the mountain states: Model analysis and observational evidence from space, J. Geophys. Res.-Atmos., 118, 12784–12803, doi:10.1002/2013jd020205, 2013.

Jenkin, M. E., Saunders, S. M., and Pilling, M. J.: The tropospheric degradation of volatile organic compounds: A protocol for mechanism development, Atmos. Environ., 31, 81–104, 1997.

Kanaya, Y., Pochanart, P., Liu, Y., Li, J., Tanimoto, H., Kato, S., Suthawaree, J., Inomata, S., Taketani, F., Okuzawa, K., Kawamura, K., Akimoto, H., and Wang, Z. F.: Rates and regimes of photochemical ozone production over Central East China in June 2006: a box model analysis using comprehensive measurements of ozone precursors, Atmos. Chem. Phys., 9, 7711–7723, doi:10.5194/acp-9-7711-2009, 2009.

Karl, T., Harley, P., Emmons, L., Thornton, B., Guenther, A., Basu, C., Turnipseed, A., and Jardine, K.: Efficient Atmospheric Cleansing of Oxidized Organic Trace Gases by Vegetation, Science, 330, 816–819, doi:10.1126/Science.1192534, 2010.

Kim, K. H., Ho, D. X., Park, C. G., Ma, C. J., Pandey, S. K., Lee, S. C., Jeong, H. J., and Lee, S. H.: Volatile Organic Compounds in Ambient Air at Four Residential Locations in Seoul, Korea, Environ. Eng. Sci., 29, 875–889, doi:10.1089/Ees.2011.0280, 2012.

Kim, S., Karl, T., Guenther, A., Tyndall, G., Orlando, J., Harley, P., Rasmussen, R., and Apel, E.: Emissions and ambient distributions of Biogenic Volatile Organic Compounds (BVOC) in a ponderosa pine ecosystem: interpretation of PTR-MS mass spectra, Atmos. Chem. Phys., 10, 1759–1771, doi:10.5194/acp-10-1759-2010, 2010.

Kim, S., Guenther, A., Karl, T., and Greenberg, J.: Contributions of primary and secondary biogenic VOC tototal OH reactivity during the CABINEX (Community Atmosphere-Biosphere INteractions Experiments)-09 field campaign, Atmos. Chem. Phys., 11, 8613–8623, doi:10.5194/acp-11-8613-2011, 2011.

Kim, S., Guenther, A., and Apel, E.: Quantitative and qualitative sensing techniques for biogenic volatile organic compounds and their oxidation products, Environ. Sci.-Proc. Imp., 15, 1301–1314, doi:10.1039/C3em00040k, 2013a.

Kim, S., Lee, M., Kim, S., Choi, S., Seok, S., and Kim, S.: Photochemical characteristics of high and low ozone episodes observed in the Taehwa Forest observatory (TFO) in June 2011 near Seoul South Korea, Asia-Pac. J. Atmos. Sci., 49, 325–331, doi:10.1007/S13143-013-0031-0, 2013b.

Kim, S., Wolfe, G. M., Mauldin, L., Cantrell, C., Guenther, A., Karl, T., Turnipseed, A., Greenberg, J., Hall, S. R., Ullmann, K., Apel, E., Hornbrook, R., Kajii, Y., Nakashima, Y., Keutsch, F. N., DiGangi, J. P., Henry, S. B., Kaser, L., Schnitzhofer, R., Graus, M., Hansel, A., Zheng, W., and Flocke, F. F.: Evaluation of HO_x sources and cycling using measurement-constrained model calculations in a 2-methyl-3-butene-2-ol (MBO) and monoterpene (MT) dominated ecosystem, Atmos. Chem. Phys., 13, 2031–2044, doi:10.5194/acp-13-2031-2013, 2013c.

Kim, S., VandenBoer, T. C., Young, C. J., Riedel, T. P., Thornton, J. A., Swarthout, B., Sive, B., Lerner, B., Gilman, J. B., Warneke, C., Roberts, J. M., Guenther, A., Wagner, N. L., Dube, W. P., Williams, E., and Brown, S. S.: The primary and recycling sources of OH during the NACHTT-2011 campaign: HONO as an important OH primary source in the wintertime, J. Geophys. Res.-Atmos., 119, 6886–6896, doi:10.1002/2013jd019784, 2014.

Kim, S. Y., Jiang, X. Y., Lee, M., Turnipseed, A., Guenther, A., Kim, J. C., Lee, S. J., and Kim, S.: Impact of biogenic volatile organic compounds on ozone production at the Taehwa Research Forest near Seoul, South Korea, Atmos. Environ., 70, 447–453, doi:10.1016/J.Atmosenv.2012.11.005, 2013.

Kleinman, L. I.: Ozone process insights from field experiments – part II: Observation-based analysis for ozone production, Atmos. Environ., 34, 2023–2033, doi:10.1016/S1352-2310(99)00457-4, 2000.

Leighton, P. A.: Photochemistry of Air Pollution, Academic, San Diego, CA USA, 1961.

Lelieveld, J., Butler, T. M., Crowley, J. N., Dillon, T. J., Fischer, H., Ganzeveld, L., Harder, H., Lawrence, M. G., Martinez, M., Taraborrelli, D., and Williams, J.: Atmospheric oxidation capacity sustained by a tropical forest, Nature, 452, 737–740, 2008.

Levy, H.: Normal Atmosphere – Large Radical and Formaldehyde Concentrations Predicted, Science, 173, 141–143, 1971.

Li, X., Brauers, T., Häseler, R., Bohn, B., Fuchs, H., Hofzumahaus, A., Holland, F., Lou, S., Lu, K. D., Rohrer, F., Hu, M., Zeng, L. M., Zhang, Y. H., Garland, R. M., Su, H., Nowak, A., Wiedensohler, A., Takegawa, N., Shao, M., and Wahner, A.: Exploring the atmospheric chemistry of nitrous acid (HONO) at a ru-

ral site in Southern China, Atmos. Chem. Phys., 12, 1497–1513, doi:10.5194/acp-12-1497-2012, 2012.

Li, Y., Lau, A. K. H., Fung, J. C. H., Zheng, J. Y., and Liu, S. C.: Importance of NO$_x$ control for peak ozone reduction in the Pearl River Delta region, J. Geophys. Res.-Atmos., 118, 9428–9443, doi:10.1002/Jgrd.50659, 2013.

Lim, Y. J., Armendariz, A., Son, Y. S., and Kim, J. C.: Seasonal variations of isoprene emissions from five oak tree species in East Asia, Atmos. Environ., 45, 2202–2210, doi:10.1016/J.Atmosenv.2011.01.066, 2011.

Liu, Y. J., Herdlinger-Blatt, I., McKinney, K. A., and Martin, S. T.: Production of methyl vinyl ketone and methacrolein via the hydroperoxyl pathway of isoprene oxidation, Atmos. Chem. Phys., 13, 5715–5730, doi:10.5194/acp-13-5715-2013, 2013.

Lou, S., Holland, F., Rohrer, F., Lu, K., Bohn, B., Brauers, T., Chang, C.C., Fuchs, H., Häseler, R., Kita, K., Kondo, Y., Li, X., Shao, M., Zeng, L., Wahner, A., Zhang, Y., Wang, W., and Hofzumahaus, A.: Atmospheric OH reactivities in the Pearl River Delta – China in summer 2006: measurement and model results, Atmos. Chem. Phys., 10, 11243–11260, doi:10.5194/acp-10-11243-2010, 2010.

Lu, K. D., Rohrer, F., Holland, F., Fuchs, H., Bohn, B., Brauers, T., Chang, C. C., Häseler, R., Hu, M., Kita, K., Kondo, Y., Li, X., Lou, S. R., Nehr, S., Shao, M., Zeng, L. M., Wahner, A., Zhang, Y. H., and Hofzumahaus, A.: Observation and modelling of OH and HO$_2$ concentrations in the Pearl River Delta 2006: a missing OH source in a VOC rich atmosphere, Atmos. Chem. Phys., 12, 1541–1569, doi:10.5194/acp-12-1541-2012, 2012.

Ma, J. Z., Wang, W., Chen, Y., Liu, H. J., Yan, P., Ding, G. A., Wang, M. L., Sun, J., and Lelieveld, J.: The IPAC-NC field campaign: a pollution and oxidization pool in the lower atmosphere over Huabei, China, Atmos. Chem. Phys., 12, 3883–3908, doi:10.5194/acp-12-3883-2012, 2012.

Mannschreck, K., Gilge, S., Plass-Duelmer, C., Fricke, W., and Berresheim, H.: Assessment of the applicability of NO-NO$_2$-O$_3$ photostationary state to long-term measurements at the Hohenpeissenberg GAW Station, Germany, Atmos. Chem. Phys., 4, 1265–1277, doi:10.5194/acp-4-1265-2004, 2004.

Mao, J., Ren, X. R., Chen, S. A., Brune, W. H., Chen, Z., Martinez, M., Harder, H., Lefer, B., Rappenglück, B., Flynn, J., and Leuchner, M.: Atmospheric oxidation capacity in the summer of Houston 2006: Comparison with summer measurements in other metropolitan studies, Atmos. Environ., 44, 4107–4115, doi:10.1016/J.Atmosenv.2009.01.013, 2010.

Mao, J., Ren, X., Zhang, L., Van Duin, D. M., Cohen, R. C., Park, J.-H., Goldstein, A. H., Paulot, F., Beaver, M. R., Crounse, J. D., Wennberg, P. O., DiGangi, J. P., Henry, S. B., Keutsch, F. N., Park, C., Schade, G. W., Wolfe, G. M., Thornton, J. A., and Brune, W. H.: Insights into hydroxyl measurements and atmospheric oxidation in a California forest, Atmos. Chem. Phys., 12, 8009–8020, doi:10.5194/acp-12-8009-2012, 2012.

Na, K. and Kim, Y. P.: Seasonal characteristics of ambient volatile organic compounds in Seoul, Korea, Atmos. Environ., 35, 2603–2614, doi:10.1016/S1352-2310(00)00464-7, 2001.

Nakashima, Y., Kato, S., Greenberg, J., Harley, P., Karl, T., Turnipseed, A., Apel, E., Guenther, A., Smith, J., and Kajii, Y.: Total OH reactivity measurements in ambient air in a southern Rocky mountain ponderosa pine forest during BEACHON-SRM08 summer campaign, Atmos. Environ., 85, 1–8, doi:10.1016/J.Atmosenv.2013.11.042, 2014.

NIER: Annual Report for Atmospheric Environment, National Insititute of Environmetal Research, Ministry of Environment of Republic of Korea, Seoul South Korea, 2010.

Nölscher, A. C., Williams, J., Sinha, V., Custer, T., Song, W., Johnson, A. M., Axinte, R., Bozem, H., Fischer, H., Pouvesle, N., Phillips, G., Crowley, J. N., Rantala, P., Rinne, J., Kulmala, M., Gonzales, D., Valverde-Canossa, J., Vogel, A., Hoffmann, T., Ouwersloot, H. G., Vilà-Guerau de Arellano, J., and Lelieveld, J.: Summertime total OH reactivity measurements from boreal forest during HUMPPA-COPEC 2010, Atmos. Chem. Phys., 12, 8257–8270, doi:10.5194/acp-12-8257-2012, 2012.

Oswald, R., Behrendt, T., Ermel, M., Wu, D., Su, H., Cheng, Y., Breuninger, C., Moravek, A., Mougin, E., Delon, C., Loubet, B., Pommerening-Roser, A., Sorgel, M., Pöschl, U., Hoffmann, T., Andreae, M. O., Meixner, F. X., and Trebs, I.: HONO Emissions from Soil Bacteria as a Major Source of Atmospheric Reactive Nitrogen, Science, 341, 1233–1235, doi:10.1126/Science.1242266, 2013.

Paulot, F., Crounse, J. D., Kjaergaard, H. G., Kroll, J. H., Seinfeld, J. H., and Wennberg, P. O.: Isoprene photooxidation: new insights into the production of acids and organic nitrates, Atmos. Chem. Phys., 9, 1479–1501, doi:10.5194/acp-9-1479-2009, 2009.

Paulson, S. E. and Seinfeld, J. H.: Development and evaluation of a photooxidation mechanism for isoprene, J. Geophys. Res., 97, 20703–20715, 1992.

Peeters, J. and Muller, J. F.: HO$_x$ radical regeneration in isoprene oxidation via peroxy radical isomerisations. II: experimental evidence and global impact, Phys. Chem. Chem. Phys., 12, 14227–14235, doi:10.1039/C0cp00811g, 2010.

Pollack, I. B., Ryerson, T. B., Trainer, M., Neuman, J. A., Roberts, J. M., and Parrish, D. D.: Trends in ozone, its precursors, and related secondary oxidation products in Los Angeles, California: A synthesis of measurements from 1960 to 2010, J. Geophys. Res.-Atmos., 118, 5893–5911, doi:10.1002/Jgrd.50472, 2013.

Ran, L., Zhao, C. S., Xu, W. Y., Lu, X. Q., Han, M., Lin, W. L., Yan, P., Xu, X. B., Deng, Z. Z., Ma, N., Liu, P. F., Yu, J., Liang, W. D., and Chen, L. L.: VOC reactivity and its effect on ozone production during the HaChi summer campaign, Atmos. Chem. Phys., 11, 4657–4667, doi:10.5194/acp-11-4657-2011, 2011.

Ren, X., Sanders, J. E., Rajendran, A., Weber, R. J., Goldstein, A. H., Pusede, S. E., Browne, E. C., Min, K.-E., and Cohen, R. C.: A relaxed eddy accumulation system for measuring vertical fluxes of nitrous acid, Atmos. Meas. Tech., 4, 2093–2103, doi:10.5194/amt-4-2093-2011, 2011.

Roberts, J. M., Veres, P., Warneke, C., Neuman, J. A., Washenfelder, R. A., Brown, S. S., Baasandorj, M., Burkholder, J. B., Burling, I. R., Johnson, T. J., Yokelson, R. J., and de Gouw, J.: Measurement of HONO, HNCO, and other inorganic acids by negative-ion proton-transfer chemical-ionization mass spectrometry (NI-PT-CIMS): application to biomass burning emissions, Atmos. Meas. Tech., 3, 981–990, doi:10.5194/amt-3-981-2010, 2010.

Ryerson, T. B., Andrews, A. E., Angevine, W. M., Bates, T. S., Brock, C. A., Cairns, B., Cohen, R. C., Cooper, O. R., de Gouw, J. A., Fehsenfeld, F. C., Ferrare, R. A., Fischer, M. L., Flagan, R. C., Goldstein, A. H., Hair, J. W., Hardesty, R. M., Hostetler, C. A., Jimenez, J. L., Langford, A. O., McCauley, E., McKeen, S.

A., Molina, L. T., Nenes, A., Oltmans, S. J., Parrish, D. D., Peder-
son, J. R., Pierce, R. B., Prather, K., Quinn, P. K., Seinfeld, J. H.,
Senff, C. J., Sorooshian, A., Stutz, J., Surratt, J. D., Trainer, M.,
Volkamer, R., Williams, E. J., and Wofsy, S. C.: The 2010 Cali-
fornia Research at the Nexus of Air Quality and Climate Change
(CalNex) field study, J. Geophys. Res.-Atmos., 118, 5830–5866,
doi:10.1002/Jgrd.50331, 2013.

Ryu, Y.-H., Baik, J.-J., Kwak, K.-H., Kim, S., and Moon, N.: Im-
pacts of urban land-surface forcing on ozone air quality in the
Seoul metropolitan area, Atmos. Chem. Phys., 13, 2177–2194,
doi:10.5194/acp-13-2177-2013, 2013.

Sartelet, K. N., Couvidat, F., Seigneur, C., and Roustan,
Y.: Impact of biogenic emissions on air quality over Eu-
rope and North America, Atmos. Environ., 53, 131–141,
doi:10.1016/J.Atmosenv.2011.10.046, 2012.

Saunders, S. M., Jenkin, M. E., Derwent, R. G., and Pilling, M.
J.: Protocol for the development of the Master Chemical Mech-
anism, MCM v3 (Part A): tropospheric degradation of non-
aromatic volatile organic compounds, Atmos. Chem. Phys., 3,
161–180, doi:10.5194/acp-3-161-2003, 2003.

Shao, M., Lu, S. H., Liu, Y., Xie, X., Chang, C. C., Huang, S., and
Chen, Z. M.: Volatile organic compounds measured in summer in
Beijing and their role in ground-level ozone formation, J. Geo-
phys. Res.-Atmos., 114, D00G06, doi:10.1029/2008jd010863,
2009a.

Shao, M., Zhang, Y. H., Zeng, L. M., Tang, X. Y., Zhang,
J., Zhong, L. J., and Wang, B. G.: Ground-level ozone
in the Pearl River Delta and the roles of VOC and
NO(x) in its production, J. Environ. Manage., 90, 512–518,
doi:10.1016/J.Jenvman.2007.12.008, 2009b.

Sillman, S. and He, D.: Some theoretical results concerning O_3-
NO_x-VOC chemistry and NO_x-VOC indicators, J. Geophys.
Res., 107, 4659, doi:10.1029/2001JD001123, 2002.

Simon, P. K. and Dasgupta, P. K.: Continuous Automated Mea-
surement of Gaseous Nitrous and Nitric-Acids and Particu-
late Nitrite and Nitrate, Environ. Sci. Technol., 29, 1534–1541,
doi:10.1021/Es00006a015, 1995.

Sinha, V., Williams, J., Lelieveld, J., Ruuskanen, T. M., Kajos, M.
K., Patokoski, J., Hellen, H., Hakola, H., Mogensen, D., Boy, M.,
Rinne, J., and Kulmala, M.: OH Reactivity Measurements within
a Boreal Forest: Evidence for Unknown Reactive Emissions,
Environ. Sci. Technol., 44, 6614–6620, doi:10.1021/Es101780b,
2010.

Song, C. H., Park, M. E., Lee, E. J., Lee, J. H., Lee, B. K., Lee,
D. S., Kim, J., Han, J. S., Moon, K. J., and Kondo, Y.: Possible
particulate nitrite formation and its atmospheric implications in-
ferred from the observations in Seoul, Korea, Atmos. Environ.,
43, 2168–2173, doi:10.1016/J.Atmosenv.2009.01.018, 2009.

Spaulding, R. S., Schade, G. W., Goldstein, A. H., and Charles,
M. J.: Characterization of secondary atmospheric photooxidation
products: Evidence for biogenic and anthropogenic sources, J.
Geophys. Res.-Atmos., 108, 4247, doi:10.1029/2002jd002478,
2003.

Steinbacher, M., Zellweger, C., Schwarzenbach, B., Bugmann, S.,
Buchmann, B., Ordonez, C., Prevot, A. S. H., and Hueglin,
C.: Nitrogen oxide measurements at rural sites in Switzerland:
Bias of conventional measurement techniques, J. Geophys. Res.-
Atmos., 112, D11307, doi:10.1029/2006jd007971, 2007.

Takeuchi, M., Li, J. Z., Morris, K. J., and Dasgupta, P. K.:
Membrane-based parallel plate denuder for the collection and
removal of soluble atmospheric gases, Anal. Chem., 76, 1204–
1210, doi:10.1021/Ac0348423, 2004.

Tie, X., Geng, F., Guenther, A., Cao, J., Greenberg, J., Zhang, R.,
Apel, E., Li, G., Weinheimer, A., Chen, J., and Cai, C.: Megac-
ity impacts on regional ozone formation: observations and WRF-
Chem modeling for the MIRAGE-Shanghai field campaign, At-
mos. Chem. Phys., 13, 5655–5669, doi:10.5194/acp-13-5655-
2013, 2013.

Tonnesen, G. S. and Dennis, R. L.: Analysis of radical propa-
gation efficiency to assess ozone sensitivity to hydrocarbons
and NO_x 1. Local indicators of instantaneous odd oxygen pro-
duction sensitivity, J. Geophys. Res.-Atmos., 105, 9213–9225,
doi:10.1029/1999jd900371, 2000a.

Tonnesen, G. S. and Dennis, R. L.: Analysis of radical propa-
gation efficiency to assess ozone sensitivity to hydrocarbons
and NO_x 2. Long-lived species as indicators of ozone concen-
tration sensitivity, J. Geophys. Res.-Atmos., 105, 9227–9241,
doi:10.1029/1999jd900372, 2000b.

Trainer, M., Williams, E., Parrish, D. D., Buhr, M. P., Allwine, E. J.,
Westberg, H., Fehsenfeld, F. C., and Liu, S. C.: Models and ob-
servations of the impact of natural hydrocarbons on rural ozone,
Nature, 329, 705–707, 1987.

Tseng, K. H., Wang, J. L., Cheng, M. T., and Tsuang, B. J.: As-
sessing the Relationship between Air Mass Age and Summer
Ozone Episodes Based on Photochemical Indices, Aerosol Air
Qual. Res., 9, 149–171, 2009.

Villena, G., Bejan, I., Kurtenbach, R., Wiesen, P., and Kleffmann, J.:
Interferences of commercial NO_2 instruments in the urban atmo-
sphere and in a smog chamber, Atmos. Meas. Tech., 5, 149–159,
doi:10.5194/amt-5-149-2012, 2012.

Wolfe, G. M. and Thornton, J. A.: The Chemistry of Atmosphere-
Forest Exchange (CAFE) Model – Part 1: Model descrip-
tion and characterization, Atmos. Chem. Phys., 11, 77–101,
doi:10.5194/acp-11-77-2011, 2011.

Wolfe, G. M., Crounse, J. D., Parrish, J. D., St Clair, J. M., Beaver,
M. R., Paulot, F., Yoon, T. P., Wennberg, P. O., and Keutsch,
F. N.: Photolysis, OH reactivity and ozone reactivity of a proxy
for isoprene-derived hydroperoxyenals (HPALDs), Phys. Chem.
Chem. Phys., 14, 7276–7286, 2012.

Wolfe, G. M., Cantrell, C., Kim, S., Mauldin III, R. L., Karl, T.,
Harley, P., Turnipseed, A., Zheng, W., Flocke, F., Apel, E. C.,
Hornbrook, R. S., Hall, S. R., Ullmann, K., Henry, S. B., Di-
Gangi, J. P., Boyle, E. S., Kaser, L., Schnitzhofer, R., Hansel,
A., Graus, M., Nakashima, Y., Kajii, Y., Guenther, A., and
Keutsch, F. N.: Missing peroxy radical sources within a summer-
time ponderosa pine forest, Atmos. Chem. Phys., 14, 4715–4732,
doi:10.5194/acp-14-4715-2014, 2014.

Wong, K. W., Tsai, C., Lefer, B., Haman, C., Grossberg, N., Brune,
W. H., Ren, X., Luke, W., and Stutz, J.: Daytime HONO vertical
gradients during SHARP 2009 in Houston, TX, Atmos. Chem.
Phys., 12, 635–652, doi:10.5194/acp-12-635-2012, 2012.

Xing, J., Wang, S. X., Jang, C., Zhu, Y., and Hao, J. M.: Nonlin-
ear response of ozone to precursor emission changes in China:
a modeling study using response surface methodology, Atmos.
Chem. Phys., 11, 5027–5044, doi:10.5194/acp-11-5027-2011,
2011.

Yoshino, A., Nakashima, Y., Miyazaki, K., Kato, S., Suthawaree, J., Shimo, N., Matsunaga, S., Chatani, S., Apel, E., Greenberg, J., Guenther, A., Ueno, H., Sasaki, H., Hoshi, J., Yokota, H., Ishii, K., and Kajii, Y.: Air quality diagnosis from comprehensive observations of total OH reactivity and reactive trace species in urban central Tokyo, Atmos Environ, 49, 51–59, doi:10.1016/J.Atmosenv.2011.12.029, 2012.

Yuan, B., Warneke, C., Shao, M., and de Gouw, J. A.: Interpretation of volatile organic compound measurements by proton-transfer-reaction mass spectrometry over the deepwater horizon oil spill, Int. J. Mass Spectrom., 358, 43–48, doi:10.1016/J.Ijms.2013.11.006, 2014.

Zhang, Y., Hu, X. M., Leung, L. R., and Gustafson, W. I.: Impacts of regional climate change on biogenic emissions and air quality, J. Geophys. Res.-Atmos., 113, D18310, doi:10.1029/2008jd009965, 2008.

Zhang, Y. H., Su, H., Zhong, L. J., Cheng, Y. F., Zeng, L. M., Wang, X. S., Xiang, Y. R., Wang, J. L., Gao, D. F., Shao, M., Fan, S. J., and Liu, S. C.: Regional ozone pollution and observation-based approach for analyzing ozone-precursor relationship during the PRIDE-PRD2004 campaign, Atmos. Environ., 42, 6203–6218, doi:10.1016/J.Atmosenv.2008.05.002, 2008.

Zhao, J. and Zhang, R. Y.: Proton transfer reaction rate constants between hydronium ion ($H_3O(+)$) and volatile organic compounds, Atmos. Environ., 38, 2177–2185, 2004.

Zhou, X. L., Zhang, N., TerAvest, M., Tang, D., Hou, J., Bertman, S., Alaghmand, M., Shepson, P. B., Carroll, M. A., Griffith, S., Dusanter, S., and Stevens, P. S.: Nitric acid photolysis on forest canopy surface as a source for tropospheric nitrous acid, Nat. Geosci., 4, 440–443, 2011.